

Solving one dimensional nonlinear coupled Burger's equations using high accuracy multiquadric quasi-interpolation

Mahbubeh Rahimi

Department of Mathematics, Central Tehran Branch,
Islamic Azad University, Tehran, Iran.
E-mail: rahimi_mah@yahoo.com

Hojatollah Adibi*

Department of Mathematics, Central Tehran Branch,
Islamic Azad University, Tehran, Iran.
E-mail: adibih@aut.ac.ir

Abstract In this paper a multiquadric quasi-interpolation (MQQI) scheme for solving the system of 1-D coupled nonlinear Burger's equations (CNBE) is presented. The scheme utilizes the derivative of the quasi-interpolation for approximating the spatial derivative and the Taylor series expansion for temporal derivatives. Simulations are presented to demonstrate the efficiency and applicability of the scheme. Also, we have shown that our scheme is superior to some numerical schemes already done.

Keywords. One dimensional coupled nonlinear Burger's equations, Multiquadric quasi-interpolation, Compact finite difference, Collocation method.

2010 Mathematics Subject Classification. 35M99, 35C99.

1. INTRODUCTION

Consider the CNBE in generalized form:

$$u_t = u_{xx} - \eta uu_x - \alpha(uv)_x, \quad a \leq x \leq b, \quad 0 \leq t \leq T, \quad (1.1)$$

$$v_t = v_{xx} - \xi vv_x - \beta(uv)_x, \quad a \leq x \leq b, \quad 0 \leq t \leq T, \quad (1.2)$$

subject to the initial conditions

$$u(x, 0) = f_1(x), \quad v(x, 0) = f_2(x), \quad (1.3)$$

and the boundary conditions

$$u(a, t) = g_a(t), \quad u(b, t) = g_b(t), \quad (1.4)$$

$$v(a, t) = h_a(t), \quad v(b, t) = h_b(t), \quad (1.5)$$

where α , β , ξ and η are constants, and $u(x, t)$, $v(x, t)$ are two unknowns. g_a , g_b , h_a and h_b are all known functions [6].

Received: 27 February 2019 ; Accepted: 21 January 2020.

* corresponding.

A numerical solution of a CNBE obtained by Esipov [7], for the model of polydisperse sedimentation. Eqs. (1.1)-(1.5) also model the sedimentation and evolution of volume concentrations of a couple of particles floated in fluid [6]. Analytical solution of 1-D system of coupled Burger's equations have been proposed by Kaya [10], using Adomian decomposition method, also Soliman [17], applied an extended tanh function method. The numerical solutions to the CNBE have been solved by many authors using different methods [1, 2, 3, 7]. Wei and Gu [19], used a conjugate filter approach, Khater [11], applied the chebyshev spectral collocation method, Dehghan [5], used Adomian-Pade technique. Rashid and Ismail [15], gave numerical solution of coupled Burger's equations by using Fourier pseudo-spectral method. Recently, Mittal and Arrora [13], has applied cubic B-spline collocation scheme, Mokhtari [14], used a generalized differential quadrature method.

In 1992, Beaton and Powell proposed three univariate MQQI named as \mathcal{L}_A , \mathcal{L}_B and \mathcal{L}_C [4]. Wu and Schaback [20], presented the MQQI operator \mathcal{L}_D . Recently, Jiang et al. [9] have presented a new multilevel univariate MQQI method based upon inverse multiquadric (IMQ) RBF interpolation and Wu and Schaback's operator \mathcal{L}_D namely as \mathcal{L}_W and \mathcal{L}_{W_2} .

In this work, we investigate the solution of the 1-D CNBE using high accuracy MQQI method based upon a linear combination of MQ basis. The most important advantage to be taken from quasi-interpolation is to evaluate the approximate solution without needing to solve any system of equations. In definition process of the quasi-interpolation \mathcal{L}_{W_2} we use compact finite difference scheme for second derivative approximation.

2. THE MQQI SCHEME

Considering the partition

$$a = x_0 < x_1 < \dots < x_n = b, \quad h = \max_{1 \leq i \leq n} (x_i - x_{i-1}), \quad (2.1)$$

on $\Omega = [a, b]$, the univariate real function f usually takes the following quasi-interpolation form

$$L(f) = \sum_{i=0}^n f(x_i) \psi_i(x), \quad x_i \in [a, b], \quad (2.2)$$

where each function $\psi_i(x)$ is a multiquadric radial basis function [8], defined by

$$\psi_i(x) = (c^2 + (x - x_i)^2)^{1/2}, \quad (2.3)$$

and $c > 0$ is a shape parameter. The MQQI operator \mathcal{L}_D introduced by Wu and Schaback as [20]

$$\mathcal{L}_D[f(x)] = \sum_{i=0}^n f(x_i) \tilde{\Phi}_i(x), \quad (2.4)$$



where

$$\begin{aligned} \tilde{\Phi}_0(x) &= \frac{1}{2} \left[1 + \frac{\psi_1(x) - (x - x_0)}{(x_1 - x_0)} \right], \\ \tilde{\Phi}_1(x) &= \frac{1}{2} \left[\frac{\psi_2(x) - \psi_1(x)}{(x_2 - x_1)} - \frac{\psi_1(x) - (x - x_0)}{(x_1 - x_0)} \right], \\ \tilde{\Phi}_i(x) &= \frac{1}{2} \left[\frac{\psi_{i+1}(x) - \psi_i(x)}{(x_{i+1} - x_i)} - \frac{\psi_i(x) - \psi_{i-1}(x)}{(x_i - x_{i-1})} \right], \quad 2 \leq i \leq n - 2, \quad (2.5) \\ \tilde{\Phi}_{n-1}(x) &= \frac{1}{2} \left[\frac{(x_n - x) - \psi_{n-1}(x)}{(x_n - x_{n-1})} - \frac{\psi_{n-1}(x) - \psi_{n-2}(x)}{(x_{n-1} - x_{n-2})} \right], \\ \tilde{\Phi}_n(x) &= \frac{1}{2} \left[1 + \frac{\psi_{n-1}(x) - (x_n - x)}{(x_n - x_{n-1})} \right]. \end{aligned}$$

Now, we choose a smaller set $\{x_{k_i}\}_{i=1}^N$ from the given points $\{x_i\}_{i=0}^n$ where $N < n$ and $0 = k_0 < k_1 < \dots < k_{N+1} = n$. If so, utilizing IMQ-RBF, the RBF interpolation of $S_{f''}$ can be represented by

$$S_{f''}(x) = \sum_{j=1}^N \lambda_j \bar{\varphi}_j(x), \quad (2.6)$$

where

$$\bar{\varphi}_j(x) = \frac{p^2}{(p^2 + (x - x_{k_j})^2)^{\frac{3}{2}}}, \quad (2.7)$$

with the shape parameter $p \in \mathbb{R}^+$. The coefficients $\{\lambda_j\}_{j=1}^N$ are uniquely determined by utilizing

$$S_{f''}(x_{k_i}) = \sum_{j=1}^N \lambda_j \bar{\varphi}_j(x_{k_i}) = f''(x_{k_i}), \quad (2.8)$$

as the interpolation condition.

Due to the solvability of eq. (2.8), [12], we get

$$\lambda = A_X^{-1} \cdot f''_X, \quad (2.9)$$

where $x = \{x_{k_1}, x_{k_2}, \dots, x_{k_N}\}$, $\lambda = [\lambda_1, \lambda_2, \dots, \lambda_N]^T$, $A_X = [\bar{\varphi}_j(x_{k_i})]$ and $f''_X = [f''(x_{k_1}), f''(x_{k_2}), \dots, f''(x_{k_N})]^T$. Now by using relation (2.9), an error function $e(x)$ is introduced by:

$$e(x) = f(x) - \sum_{i=1}^N \lambda_i \sqrt{p^2 + (x - x_{k_i})^2}. \quad (2.10)$$

If so, the operator \mathcal{L}_{W_2} by utilizing \mathcal{L}_D operator in relation (2.4) and (2.5) on $\{(x_i, e(x_i))\}_{i=0}^n$ is defined by [16],

$$\mathcal{L}_{W_2} f(x) = \sum_{j=1}^N \lambda_j \sqrt{p^2 + (x - x_{k_j})^2} + \mathcal{L}_D e(x), \quad (2.11)$$



in which the constants c and p as shape parameters are not the same as in relation (2.11). Now from relation (2.8) $f''(x_{k_i})$ can be written by

$$f''(x_{k_i}) = \frac{\delta_x^2}{h_2^2(1 + 12\delta_x^2)} f(x_{k_i}), \quad \text{with } h_2 = \frac{b - a}{N}, \tag{2.12}$$

where $\delta_x^2 f(x_{k_i}) = f(x_{k_{i+1}}) - 2f(x_{k_i}) + f(x_{k_{i-1}})$ which yields

$$\sum_{j=1}^N \lambda_j \bar{\varphi}_j(x_{k_i}) = \frac{\delta_x^2}{h_2^2(1 + 12\delta_x^2)} f(x_{k_i}), \quad 1 \leq i \leq N. \tag{2.13}$$

As a result, the coefficients $\{\lambda_j\}_{j=1}^N$ are determined uniquely, via the linear system

$$\lambda = A_X^{*-1} \cdot f_X'', \tag{2.14}$$

where $A_X^* = [(1 + 12\delta_x^2)\bar{\varphi}_j(x_{k_i})]$. The accuracy and properties of \mathcal{L}_W and \mathcal{L}_{W_2} , have been discussed in [9]. Now we use of MQQI operator \mathcal{L}_{W_2} and equally spaced points. The compact form of operator \mathcal{L}_{W_2} can be represented as [16]:

$$\mathcal{L}_{W_2} f(x) = \sum_{i=0}^n f(x_i) \hat{\psi}_i(x). \tag{2.15}$$

3. MESHELSS METHOD FOR THE SOLUTION OF 1-D CNBE

Let us consider the generalized form of 1-D CNBE:

$$u_t = u_{xx} - \eta u u_x - \alpha (uv)_x, \quad a \leq x \leq b, \quad 0 \leq t \leq T, \tag{3.1}$$

$$v_t = v_{xx} - \xi v v_x - \beta (uv)_x, \quad a \leq x \leq b, \quad 0 \leq t \leq T, \tag{3.2}$$

with the initial condition:

$$u(x, 0) = f_1(x), \quad v(x, 0) = f_2(x), \tag{3.3}$$

and the Dirichlet boundary condtions:

$$u(a, t) = g_a(t), \quad u(b, t) = g_b(t), \tag{3.4}$$

$$v(a, t) = h_a(t), \quad v(b, t) = h_b(t). \tag{3.5}$$

At first we discretize the temporal derivative u_t of eq. (3.1) by using Taylor series expansion. Here, the term $u_t^m = u_t(x, t_m)$ is obtained via the Taylor series expansion as

$$u_t^m = \frac{u^{m+1} - u^m}{\Delta t} - \frac{\Delta t}{2} u_{tt}^m + O(\Delta t^2). \tag{3.6}$$

Differentiating eq. (3.1) with respect to time, u_{tt}^m is deduced as:

$$\begin{aligned} u_{tt}^m = \left(u_{xx}^m - \eta u^m u_x^m - \alpha (u^m v^m)_x \right)_t &= (u_t^m)_{xx} - \eta u_t^m u_x^m \\ &\quad - \eta u^m (u_t^m)_x - \alpha (u_t^m)_x v^m \\ &\quad - \alpha u_x^m v_t^m - \alpha u_t^m v_x^m - \alpha u^m (v_t^m)_x. \end{aligned} \tag{3.7}$$



For the time derivative u_t^m in eq. (3.7), using forward difference formula, we deduce:

$$\begin{aligned} \Delta t u_{tt}^m &= \left(u_{xx}^{m+1} - u_{xx}^m \right) - \eta u_x^m \left(u^{m+1} - u^m \right) \\ &\quad - \eta u^m \left(u_x^{m+1} - u_x^m \right) - \alpha v^m \left(u_x^{m+1} - u_x^m \right) \\ &\quad - \alpha u_x^m \left(v^{m+1} - v^m \right) - \alpha v_x^m \left(u^{m+1} - u^m \right) - \alpha u^m \left(v_x^{m+1} - v_x^m \right). \end{aligned} \tag{3.8}$$

Substituting eq. (3.8) into eq. (3.6) and using the expression (3.1), yield the following time discretized form of Burger's equation (3.1):

$$\begin{aligned} u^m + \frac{\Delta t}{2} u_{xx}^m &= u^{m+1} - \frac{\Delta t}{2} u_{xx}^{m+1} - \frac{\Delta t}{2} \eta u_x^m u^{m+1} \\ &\quad - \frac{\Delta t}{2} \eta u_x^{m+1} u^m - \frac{\Delta t}{2} \alpha u_x^{m+1} v^m \\ &\quad - \frac{\Delta t}{2} \alpha u_x^m v^{m+1} - \frac{\Delta t}{2} \alpha u^{m+1} v_x^m - \frac{\Delta t}{2} \alpha u^m v_x^{m+1}. \end{aligned} \tag{3.9}$$

Also, eq. (3.2) in the form of time discretized will be as:

$$\begin{aligned} v^m + \frac{\Delta t}{2} v_{xx} &= v^{m+1} - \frac{\Delta t}{2} v_{xx}^{m+1} - \frac{\Delta t}{2} \xi v_x^m v^{m+1} \\ &\quad - \frac{\Delta t}{2} \xi v_x^{m+1} v^m - \frac{\Delta t}{2} \beta u_x^{m+1} v^m \\ &\quad - \frac{\Delta t}{2} \beta u_x^m v^{m+1} - \frac{\Delta t}{2} \beta u^{m+1} v_x^m - \frac{\Delta t}{2} \beta u^m v_x^{m+1}. \end{aligned} \tag{3.10}$$

In this scheme, u^m and v^m are approximated by:

$$u^m(x) = \sum_{i=0}^n u^m(x_i) \hat{\psi}_i(x), \tag{3.11}$$

$$v^m(x) = \sum_{i=0}^n v^m(x_i) \hat{\psi}_i(x). \tag{3.12}$$

In this scheme, $u^m(x)$ and $v^m(x)$ and their spatial derivatives u_x^m , u_{xx}^m , v_x^m and v_{xx}^m are approximated as follows:

$$\begin{aligned} u(x, t_m) &= \sum_{i=0}^n u^m(x_i) \hat{\psi}_i(x), & v(x, t_m) &= \sum_{i=0}^n v^m(x_i) \hat{\psi}_i(x), \\ u_x(x, t_m) &= \sum_{i=0}^n u^m(x_i) \check{\psi}_i(x), & v_x(x, t_m) &= \sum_{i=0}^n v^m(x_i) \check{\psi}_i(x), \\ u_{xx}(x, t_m) &= \sum_{i=0}^n u^m(x_i) \bar{\psi}_i(x), & v_{xx}(x, t_m) &= \sum_{i=0}^n v^m(x_i) \bar{\psi}_i(x), \end{aligned} \tag{3.13}$$

where

$$\frac{\partial \hat{\psi}_i}{\partial x} = \check{\psi}_i, \quad \frac{\partial^2 \hat{\psi}_i}{\partial x^2} = \bar{\psi}_i.$$



At the end, by substituting the above approximation (3.11-3.13), into eqs. (3.9) and (3.10) and boundary conditions and applying collocation method yields the following matrix forms:

$$\begin{aligned}
& \left(A_b + A_d - \frac{\Delta t}{2} C - \frac{\Delta t}{2} \eta [(BU^m) * A_d] - \frac{\Delta t}{2} \eta [(A_d U^m) * B] \right. \\
& \quad \left. - \frac{\Delta t}{2} \alpha [(A_d V^m) * B] - \alpha \frac{\Delta t}{2} [(BV^m) * A_d] \right) U^{m+1} \\
& + \left(- \frac{\Delta t}{2} \alpha [(BU^m) * A_d] - \frac{\Delta t}{2} \alpha [(A_d U^m) * B] \right) V^{m+1} \\
& = (A_d + \frac{\Delta t}{2} C) U^m + G^{m+1}, \\
& \left(- \beta \frac{\Delta t}{2} [(A_d V^m) * B] - \beta \frac{\Delta t}{2} [(BV^m) * A_d] \right) U^{m+1} \\
& + \left(A_b + A_d - \frac{\Delta t}{2} C - \frac{\Delta t}{2} \xi [(BV^m) * A_d] - \frac{\Delta t}{2} \xi [(A_d V^m) * B] \right. \\
& \quad \left. - \frac{\Delta t}{2} \beta [(A_d U^m) * B] - \frac{\Delta t}{2} \beta [(BU^m) * A_d] \right) V^{m+1} \\
& = (A_d + \frac{\Delta t}{2} C) V^m + H^{m+1}, \tag{3.14}
\end{aligned}$$

$$\begin{aligned}
A_b &= \begin{bmatrix} \hat{\psi}_{00} & \hat{\psi}_{10} & \cdots & \hat{\psi}_{n0} \\ 0 & 0 & \cdots & 0 \\ \vdots & \vdots & \ddots & \vdots \\ 0 & 0 & \cdots & 0 \\ \hat{\psi}_{0n} & \hat{\psi}_{1n} & \cdots & \hat{\psi}_{nn} \end{bmatrix}, \\
A_d &= \begin{bmatrix} 0 & 0 & \cdots & 0 \\ \hat{\psi}_{01} & \hat{\psi}_{11} & \cdots & \hat{\psi}_{n1} \\ \vdots & \vdots & \ddots & \vdots \\ \hat{\psi}_{0(n-1)} & \hat{\psi}_{1(n-1)} & \cdots & \hat{\psi}_{n(n-1)} \\ 0 & 0 & \cdots & 0 \end{bmatrix}, \\
B &= \begin{bmatrix} 0 & 0 & \cdots & 0 \\ \check{\psi}_{01} & \check{\psi}_{11} & \cdots & \check{\psi}_{n1} \\ \vdots & \vdots & \ddots & \vdots \\ \check{\psi}_{0(n-1)} & \check{\psi}_{1(n-1)} & \cdots & \check{\psi}_{n(n-1)} \\ 0 & 0 & \cdots & 0 \end{bmatrix}, \\
C &= \begin{bmatrix} 0 & 0 & \cdots & 0 \\ \bar{\psi}_{01} & \bar{\psi}_{11} & \cdots & \bar{\psi}_{n1} \\ \vdots & \vdots & \ddots & \vdots \\ \bar{\psi}_{0(n-1)} & \bar{\psi}_{1(n-1)} & \cdots & \bar{\psi}_{n(n-1)} \\ 0 & 0 & \cdots & 0 \end{bmatrix},
\end{aligned}$$



$$G^{m+1} = \begin{bmatrix} g_a(t^{m+1}) \\ 0 \\ \vdots \\ 0 \\ g_b(t^{m+1}) \end{bmatrix}, \quad H^{m+1} = \begin{bmatrix} h_a(t^{m+1}) \\ 0 \\ \vdots \\ 0 \\ h_b(t^{m+1}) \end{bmatrix},$$

$$U^{m+1} = \begin{bmatrix} u^{m+1}(x_0) \\ u^{m+1}(x_1) \\ \vdots \\ u^{m+1}(x_n) \end{bmatrix}, \quad V^{m+1} = \begin{bmatrix} v^{m+1}(x_0) \\ v^{m+1}(x_1) \\ \vdots \\ v^{m+1}(x_n) \end{bmatrix},$$

where

$$\hat{\psi}_{ij} = \hat{\psi}_i(x_j), \quad \check{\psi}_{ij} = \check{\psi}_i(x_j), \quad \bar{\psi}_{ij} = \bar{\psi}_i(x_j).$$

$$M_1 = A_b + A_d - \frac{\Delta t}{2}C - \frac{\Delta t}{2}\eta \left[(BU^m) * A_d \right] - \frac{\Delta t}{2}\eta \left[(A_dU^m) * B \right]$$

$$- \frac{\Delta t}{2}\alpha \left[(A_dV^m) * B \right] - \alpha \frac{\Delta t}{2} \left[(BV^m) * A_d \right],$$

$$N_1 = -\frac{\Delta t}{2}\alpha \left[(BU^m) * A_d \right] - \frac{\Delta t}{2}\alpha \left[(A_dU^m) * B \right],$$

$$M_2 = -\beta \frac{\Delta t}{2} \left[(A_dV^m) * B \right] - \beta \frac{\Delta t}{2} \left[(BV^m) * A_d \right],$$

$$N_2 = A_b + A_d - \frac{\Delta t}{2}C - \frac{\Delta t}{2}\xi \left[(BV^m) * A_d \right] - \frac{\Delta t}{2}\xi \left[(A_dV^m) * B \right]$$

$$- \frac{\Delta t}{2}\beta \left[(A_dU^m) * B \right] - \frac{\Delta t}{2}\beta \left[(BU^m) * A_d \right],$$

$$k_1 = A_d + \frac{\Delta t}{2}C.$$

If so, we have

$$M_1U^{m+1} + N_1V^{m+1} = k_1U^m + G^{m+1}, \tag{3.15}$$

$$M_2U^{m+1} + N_2V^{m+1} = k_1V^m + H^{m+1}, \tag{3.16}$$

which is simplified as

$$\begin{bmatrix} M_1 & N_1 \\ M_2 & N_2 \end{bmatrix} \begin{bmatrix} U^{m+1} \\ V^{m+1} \end{bmatrix} = \begin{bmatrix} k_1 & 0 \\ 0 & k_1 \end{bmatrix} \begin{bmatrix} U^m \\ V^m \end{bmatrix} + \begin{bmatrix} G^{m+1} \\ H^{m+1} \end{bmatrix},$$

where

$$M = \begin{bmatrix} M_1 & N_1 \\ M_2 & N_2 \end{bmatrix}, \quad W^{m+1} = \begin{bmatrix} U^{m+1} \\ V^{m+1} \end{bmatrix},$$

$$L = \begin{bmatrix} k_1 & 0 \\ 0 & k_1 \end{bmatrix}, \quad D^{m+1} = \begin{bmatrix} G^{m+1} \\ H^{m+1} \end{bmatrix},$$

$$MW^{m+1} = LW^m + D^{m+1},$$

$$W^{m+1} = M^{-1}LW^m + M^{-1}D^{m+1}. \tag{3.17}$$



By solving this system (3.17), we obtain approximate solution for the one dimensional coupled Burger’s equations.

4. STABILITY ANALYSIS

Now we use of spectral radius $\rho(E)$ of the amplification matrix for investigating the stability of the presented method. Let W be the exact, \tilde{W} the numerical solution and $\varepsilon^{m+1} = W^{m+1} - \tilde{W}^{m+1}$. The error vector of eqs. (1.1) and (1.2), which can be written as

$$\varepsilon^{m+1} = M^{-1}L\varepsilon^m = E\varepsilon^m, \tag{4.1}$$

where $E = M^{-1}L$. If so, for stability issue, it is needed that $\varepsilon^m \rightarrow 0$ as $m \rightarrow \infty$, i.e. $\rho(E) \leq 1$.

Now, the stability condition is satisfied if

$$\left| \frac{\eta_L}{\eta_M} \right| \leq 1, \tag{4.2}$$

where η_L and η_M are the eigenvalues of the matrices L and M respectively.

5. NUMERICAL EXPERIMENTS AND DISCUSSIONS

During this section, we examine three test problems, to show the efficiency of the scheme. We consider the following error norms [13]:

$$L_\infty = \max_{0 \leq j \leq n} |u(x_j, t) - u^*(x_j, t)|, \tag{5.1}$$

and

$$L_2 = \frac{(\sum_{j=0}^n |u(x_j, t) - u^*(x_j, t)|^2)^{1/2}}{(\sum_{j=0}^n |u(x_j, t)|^2)^{1/2}}.$$

Here $u(x_j, t)$ and $u^*(x_j, t)$ are the exact and obtained numerical solutions, respectively.

Example 5.1. In this example, $\eta = \xi = 2$. If so, the eqs. (1.1) and (1.2) are written by:

$$u_t = u_{xx} - 2uu_x - \alpha(uv)_x, \tag{5.2}$$

$$v_t = v_{xx} - 2vv_x - \beta(uv)_x. \tag{5.3}$$

The exact solutions to the eqs. (5.2) and (5.3) are [10]:

$$\left. \begin{aligned} u(x, t) &= a_0 - 2a_0A\left(\frac{2\alpha - 1}{4\alpha\beta - 1}\right) \tanh(A(x - 2At)) \\ v(x, t) &= \left(\frac{2a_0\beta - a_0}{2\alpha - 1}\right) - 2a_0A\left(\frac{2\alpha - 1}{4\alpha\beta - 1}\right) \tanh(A(x - 2At)) \end{aligned} \right\}, \tag{5.4}$$

with $-10 \leq x \leq 10$ and $t > 0$ where $A = a_0 \frac{(4\alpha\beta - 1)}{(4\alpha - 2)}$ and a_0, α and β are arbitrary constants.



The boundary and initial conditions are derived from relation (5.4). The computations are calculated in $[-10, 10]$, $\Delta t = 0.01$ and the number of partitions = 100 and $c = 8.15e - 9$, $p = 2c$. The calculated L_2 and L_∞ errors are compared in Table 1 and 2 with those already available in the literature.

The tables show the superiority of the current method to [18] and [13] in accuracy point of view.

Also, in Figure 1 the numerical solutions for $t = 1$, $\Delta t = 0.1$, $\alpha = 1$, $\beta = 2$ and number of partitions 10 are compared with relation (5.4) and evidently excellent agreement is seen between the approximate and analytical results.

TABLE 1. Comparisons between errors at different times for $u(x, t)$ for Example 5.1.

| t | α | β | MQQI | | Srivastava [18] | | Mittal [13] | |
|-----|----------|---------|----------|------------|-----------------|------------|-------------|------------|
| | | | L_2 | L_∞ | L_2 | L_∞ | L_2 | L_∞ |
| 0.5 | 0.1 | 0.3 | 2.464e-6 | 2.119e-7 | 4.028e-4 | 2.640e-5 | 6.736e-4 | 4.167e-5 |
| | 0.1 | 0.03 | 3.716e-6 | 3.155e-7 | 3.918e-4 | 2.621e-5 | 7.326e-4 | 4.590e-5 |
| 1 | 0.1 | 0.3 | 4.914e-6 | 4.221e-7 | 7.931e-4 | 5.203e-5 | 1.325e-3 | 8.258e-5 |
| | 0.1 | 0.03 | 7.413e-6 | 6.288e-7 | 7.713e-4 | 5.167e-5 | 1.452e-3 | 9.182e-5 |

TABLE 2. Comparisons between errors at different times for $v(x, t)$ for Example 5.1.

| t | α | β | MQQI | | Srivastava [18] | | Mittal [13] | |
|-----|----------|---------|----------|------------|-----------------|------------|-------------|------------|
| | | | L_2 | L_∞ | L_2 | L_∞ | L_2 | L_∞ |
| 0.5 | 0.1 | 0.3 | 4.928e-6 | 2.118e-7 | 2.214e-4 | 1.041e-5 | 9.057e-4 | 1.480e-4 |
| | 0.1 | 0.03 | 3.163e-6 | 3.155e-7 | 4.252e-4 | 3.072e-5 | 1.591e-4 | 5.729e-4 |
| 1 | 0.1 | 0.3 | 9.827e-6 | 4.221e-7 | 4.246e-4 | 1.975e-5 | 1.251e-3 | 4.770e-5 |
| | 0.1 | 0.03 | 6.309e-6 | 6.288e-7 | 8.378e-4 | 6.095e-5 | 2.250e-3 | 3.617e-4 |

Example 5.2. In this test problem, we take parameters values as $\eta = \xi = -2$, $\alpha = \beta = 1$, for which the eqs. (1.1) and (1.2) gets replaced by

$$u_t = u_{xx} + 2uu_x - (uv)_x, \tag{5.5}$$

$$v_t = v_{xx} + 2vv_x - (uv)_x. \tag{5.6}$$

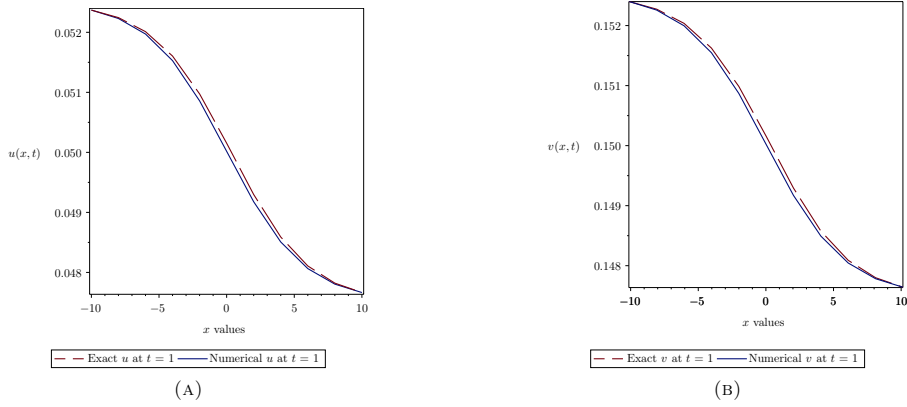
The boundary and initial conditions have been derived from the exact solutions [6]:

$$\left. \begin{aligned} u(x, t) &= \exp(-t) \sin(x) \\ v(x, t) &= \exp(-t) \sin(x) \end{aligned} \right\}, \quad -\pi \leq x \leq \pi, \quad t > 0. \tag{5.7}$$

The numerical results in $[-\pi, \pi]$ and $\Delta t = 0.001$, $c = 0.0512$ and $p = 2c$ have been shown in Tables 3 and 4 for different number of partitions and different time level. From the Tables 3 and 4, it is seen that there exists a consistency between the proposed method and exact solutions. Moreover, as the number of partitions increase the errors



FIGURE 1. Comparison between numerical and exact solutions for example 5.1.



reduce. In Figure 2 a comparison between numerical and exact solutions has been shown.

TABLE 3. Comparisons of error with $\Delta t = 0.001$ and number of partition = 200 for $u(x, t)$ in Example 5.2.

| t | MQQI | | Srivastava[18] | | Mittal[13] | |
|-----|-----------|------------|----------------|------------|------------|------------|
| | L_2 | L_∞ | L_2 | L_∞ | L_2 | L_∞ |
| 0.1 | 7.0646e-4 | 1.2830e-3 | 9.95e-4 | 9.02e-4 | 8.21e-6 | 7.45e-6 |
| 0.5 | 7.2695e-4 | 9.2818e-4 | 9.91e-4 | 6.04e-4 | 2.49e-5 | 4.10e-5 |
| 1 | 7.5127e-4 | 6.0356e-4 | 9.83e-4 | 3.65e-4 | 3.00e-5 | 8.21e-5 |

TABLE 4. Comparisons of error with $\Delta t = 0.001$ and number of partition = 400 for $u(x, t)$ in Example 5.2.

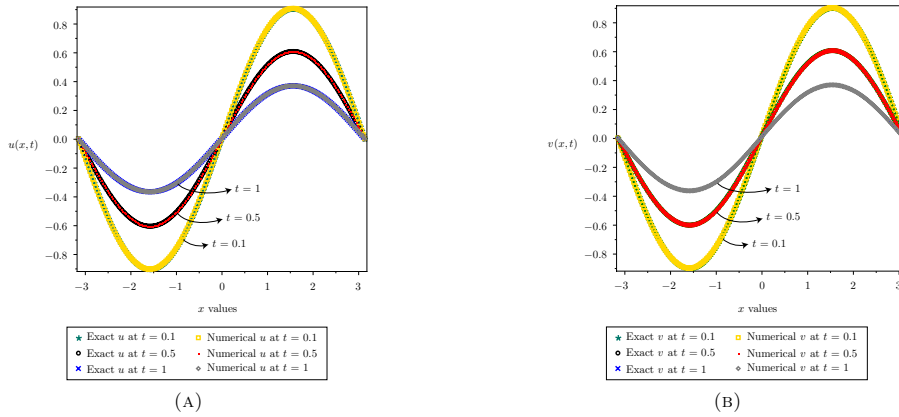
| t | MQQI | | Srivastava[18] | | Mittal[13] | |
|-----|-----------|------------|----------------|------------|------------|------------|
| | L_2 | L_∞ | L_2 | L_∞ | L_2 | L_∞ |
| 0.1 | 6.8160e-4 | 1.2031e-3 | 9.87e-4 | 8.95e-6 | 2.05e-6 | 1.86e-6 |
| 0.5 | 6.9574e-4 | 8.2786e-4 | 9.84e-4 | 6.01e-4 | 1.02e-5 | 6.22e-6 |
| 1 | 6.9964e-4 | 5.0742e-4 | 9.70e-4 | 3.64e-4 | 2.04e-5 | 7.56e-6 |

Example 5.3. We propose to compute the numerical solutions of eqs. (1.1) and (1.2) with [13]:

$$u(x, 0) = \begin{cases} \sin(2\pi x), & x \in [0, 0.5], \\ 0, & x \in (0.5, 1], \end{cases} \tag{5.8}$$



FIGURE 2. Comparison between exact and numerical solutions (A) u and (B) v in example 5.2.



$$v(x, 0) = \begin{cases} 0, & x \in [0, 0.5], \\ -\sin(2\pi x), & x \in (0.5, 1], \end{cases} \quad (5.9)$$

and $u = v = 0$, on the boundary. The solutions have been computed in $[0, 1]$ with $\Delta t = 0.001$ with 50 partitions and $c = 0.00815$, $p = 2c$. Maximum values of u and v at different time levels $t = 0.1, 0.2, 0.3, 0.4$ with $\alpha = \beta = 10$ and $\alpha = \beta = 100$ have been shown in Tables 5 and 6 for $\eta = \xi = 2$. Figures (3-6) show the computed results obtained for $\alpha = \beta = 10$ and $\alpha = \beta = 100$ for u and v , respectively when $\eta = \xi = 2$. A sharp decay has been observed in the computed solution when α and β get higher.

TABLE 5. Maximum values of u and v at different times for $\alpha = \beta = 10$ for Example 5.3.

| t | MQQI | | | | Mittal [13] | | | |
|-----|------------------|----------|------------------|----------|------------------|----------|------------------|----------|
| | max value of u | At point | max value of v | At point | max value of u | At point | max value of v | At point |
| 0.1 | 0.08313 | 0.54 | 0.11271 | 0.54 | 0.14456 | 0.58 | 0.14306 | 0.66 |
| 0.2 | 0.01332 | 0.56 | 0.02408 | 0.54 | 0.05237 | 0.54 | 0.04697 | 0.56 |
| 0.3 | 0.00188 | 0.18 | 0.00481 | 0.56 | 0.01932 | 0.52 | 0.01725 | 0.52 |
| 0.4 | 0.00015 | 0.14 | 0.00086 | 0.54 | 0.00718 | 0.50 | 0.00641 | 0.50 |



TABLE 6. Maximum values of u and v at different times for $\alpha = \beta = 100$ for Example 5.3.

| t | MQQI | | | | Mittal [13] | | | |
|-----|------------------|----------|------------------|----------|------------------|----------|------------------|----------|
| | max value of u | At point | max value of v | At point | max value of u | At point | max value of v | At point |
| 0.1 | 0.00316 | 0.06 | 0.01749 | 0.66 | 0.04175 | 0.46 | 0.05065 | 0.76 |
| 0.2 | 6.166e-6 | 0.78 | 0.00354 | 0.66 | 0.014975 | 0.58 | 0.01033 | 0.64 |
| 0.3 | 1.637e-6 | 0.78 | 0.00093 | 0.66 | 0.00534 | 0.54 | 0.00350 | 0.56 |
| 0.4 | 4.333e-7 | 0.78 | 0.00024 | 0.66 | 0.00198 | 0.52 | 0.00129 | 0.52 |

FIGURE 3. The numerical solution u of Example 5.3 at different times for $\alpha = \beta = 10, \eta = \xi = 2$.

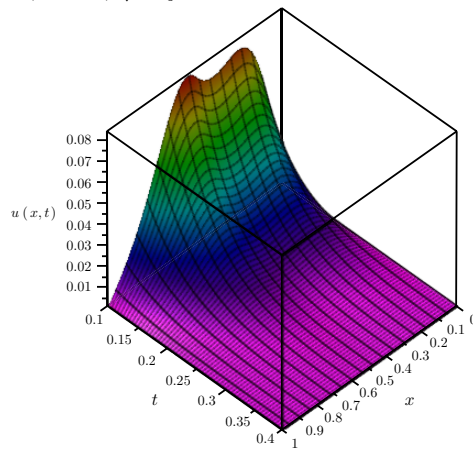


FIGURE 8. The numerical solution u in Example 5.3 for $\eta = \xi = 200$.

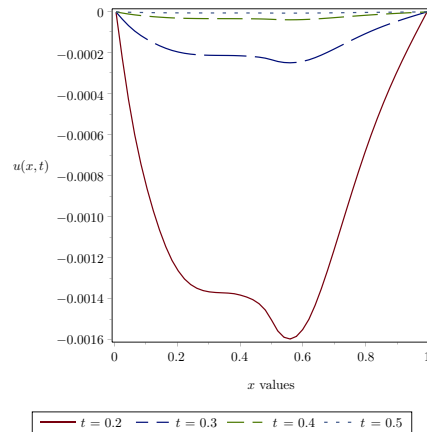


FIGURE 4. The numerical solution v of Example 5.3 at different times for $\alpha = \beta = 10, \eta = \xi = 2$.

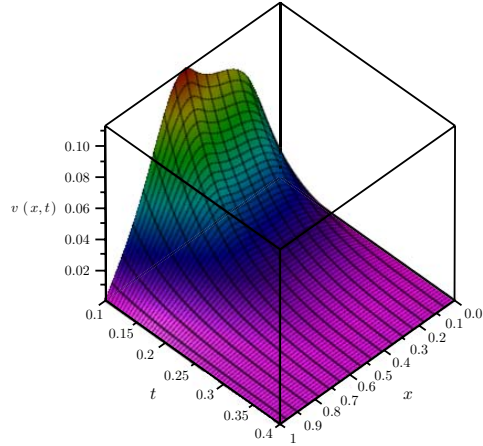
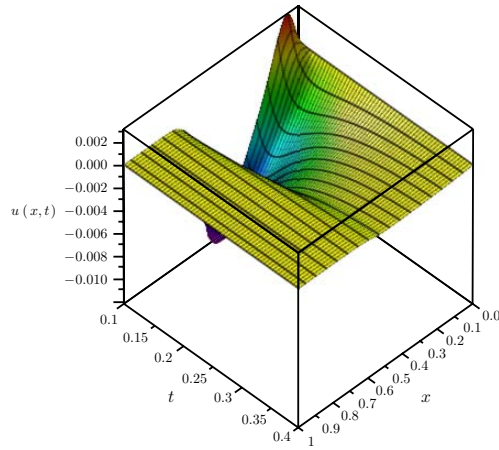


FIGURE 5. The numerical solution u in Example 5.3 at different times for $\alpha = \beta = 100, \eta = \xi = 2$.



Figures (7-12) show the calculated numerical solutions for u where $\eta = \xi = 20, 200, 2000$ with $\alpha = \beta = 10$.



FIGURE 6. The numerical solution v in Example 5.3 at different times for $\alpha = \beta = 100, \eta = \xi = 2$.

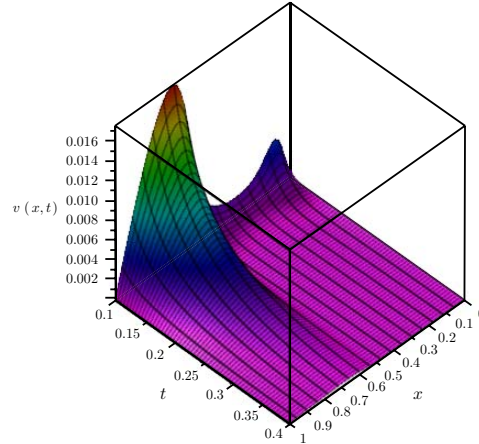


FIGURE 7. The numerical solution u in Example 5.3 for $\eta = \xi = 20$.

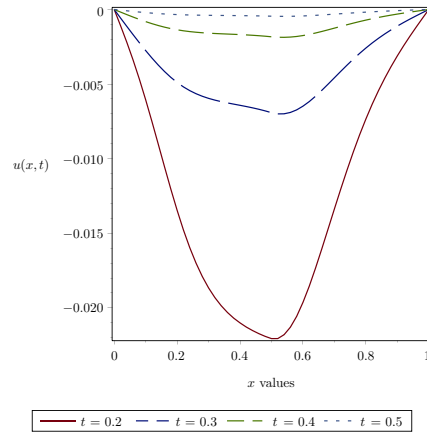


FIGURE 9. The numerical solution u in Example 5.3 for $\eta = \xi = 2000$.

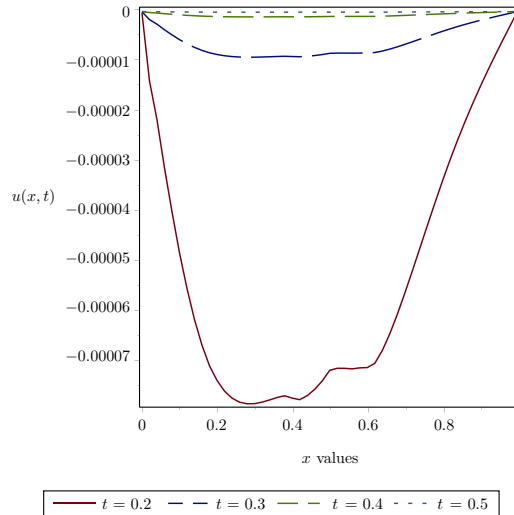


FIGURE 10. The numerical solution v in Example 5.3 for $\eta = \xi = 20$.

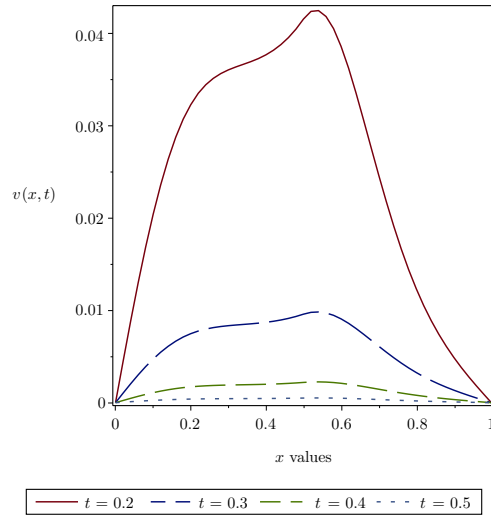


FIGURE 11. The numerical solution v in Example 5.3 for $\eta = \xi = 200$.

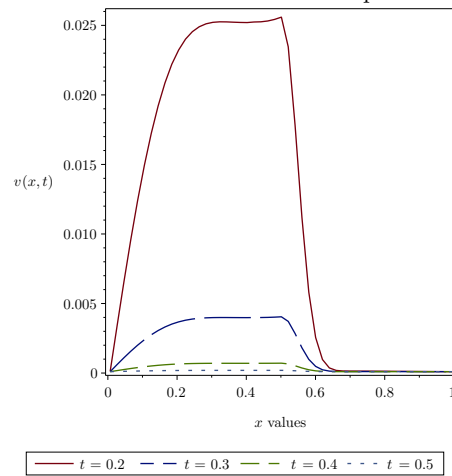
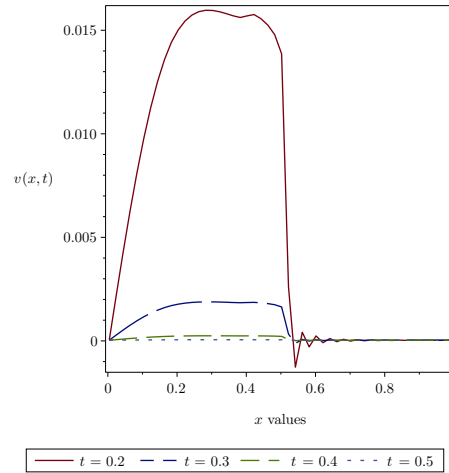


FIGURE 12. The numerical solution v in Example 5.3 for $\eta = \xi = 2000$.

It is seen from these figures that the numerical solution decays to zero as time levels and η and ξ increase.

CONCLUSIONS

In this paper a numerical approximation has been proposed for solving 1-D CNBE using a MQQI \mathcal{L}_{W_2} based on Jiang et. al [9] MQQI scheme and compact finite difference scheme. The efficiency and accuracy of the proposed scheme have been demonstrated through the three examples. The proposed method is highly accurate as compared with the other numerical schemes which are in agreement with exact solution.

REFERENCES

- [1] M. Abdou and A. Soliman, *Variational iteration method for solving burger's and coupled Burger's equations*, Journal of Computational and Applied Mathematics, 181(2) (2005),245-251.
- [2] B. Albuohimad and H. Adibi, *The Chebyshev collocation solution of the time fractional coupled Burger's equation*, Journal of Mathematics and Computer Science-JMCS, 17(1) (2017), 179-193.
- [3] B. Albuohimad and H. Adibi, *On a hybrid spectral exponential chebyshev method for time-fractional coupled Burgers equations on a semi-infinite domain*, Advances in Difference Equations, 2017(1) (2017), 85.
- [4] R. Beatson and M. Powell, *Univariate multiquadric approximation: quasi-interpolation to scattered data*, Constructive Approximation, 8(3) (1992), 275-288.
- [5] M. Dehghan, A. Hamidi, and M. Shakourifar, *The solution of coupled Burgers' equations using Adomian Pade technique*, Applied Mathematics and Computation, 189(2) (2007), 1034-1047.
- [6] J. Duan and J. Nee, *Limit set of trajectories of the coupled viscous Burger's equations*, arXiv preprint chao-dyn/9607016, 1996.



- [7] S. E. Esipov, *Coupled burgers equations: A model of polydispersive sedimentation*, Physical Review E, *52*(4) (1995), 3711.
- [8] R. L. Hardy, *Multiquadric equations of topography and other irregular surfaces*, Journal of geophysical research, *76*(8) (1971), 1905-1915.
- [9] Z. W. Jiang, R.-H. Wang, C.-G. Zhu, and M. Xu, *High accuracy multiquadric quasi- interpolation*, Applied Mathematical Modelling, *35*(5) (2011), 2185-2195.
- [10] D. Kaya, *An explicit solution of coupled viscous Burger's equation by the decomposition method*, International Journal of Mathematics and Mathematical Sciences, *27*(11) (2001), 675-680 .
- [11] A. Khater, R. Tamsah, and M. Hassan, *A chebyshev spectral collocation method for solving Burgers' type equations*, Journal of Computational and Applied Mathematics, *222*(2) (2008), 333-350.
- [12] W. Madych and S. Nelson, *Multivariate interpolation and conditionally positive definite functions*, II. Mathematics of Computation, *54*(189) (1990), 211-230.
- [13] R. Mittal and G. Arora, *Numerical solution of the coupled viscous Burger's equation*, Communications in Nonlinear Science and Numerical Simulation, *16*(3) (2011), 1304-1313.
- [14] R. Mokhtari, A. S. Toodar, and N. Chegini, *Application of the generalized differential quadrature method in solving Burger's equations*, Communications in Theoretical Physics, *56*(6) (2011), 1009.
- [15] A. Rashid and A. I. B. M. Ismail, *A fourier pseudospectral method for solving coupled viscous burgers equations*, Computational Methods in Applied Mathematics Comput. Methods Appl. Math, *9*(4) (2009), 412-420.
- [16] M. Sarboland and A. Aminataei, *On the numerical solution of one-dimensional nonlinear nonhomogeneous Burger's equation*, Journal of Applied Mathematics, 2014.
- [17] A. Soliman, *The modified extended tanh-function method for solving burgers-type equations*, Physica A: Statistical Mechanics and its Applications, *361*(2) (2006), 394-404.
- [18] V. K. Srivastava, M. Tamsir, M. K. Awasthi, and S. Singh, *One-dimensional coupled Burger's equation and its numerical solution by an implicit logarithmic finite-difference method*, Aip Advances, *4*(3) (2014), 037119.
- [19] G. Wei and Y. Gu, *Conjugate filter approach for solving Burgers' equation*, Journal of Computational and Applied Mathematics, *149*(2) (2002), 439-456.
- [20] Z. Wu and S. Robert, *Shape preserving properties and convergence of univariate multiquadric quasi-interpolation*, Acta Mathematicae Applicatae Sinica, *10*(4) (1994), 441-446.

